Role of multilevel states on quantum-dot emission in photonic-crystal cavities

K. H. Madsen, T. B. Lehmann, and P. Lodahl*

Niels Bohr Institute, University of Copenhagen, Blegdamsvej 17, DK-2100 Copenhagen, Denmark

(Received 12 February 2016; revised manuscript received 30 September 2016; published 2 December 2016)

Semiconductor quantum dots embedded in photonic-crystal nanostructures have been the subject of intense study. In this context, quantum dots are often considered to be simple two-level emitters, i.e., the complexities arising from the internal fine structure are neglected. We show that due to the intricate spatial variations of the electric field polarization found in photonic crystal, the two orthogonal fine-structure states of quantum dots in general both couple significantly to a cavity mode, implying that the two-level description is not sufficient. As a consequence the emission dynamics and spectra, which are often recorded in experiments, are modified both in the weak- and strong-coupling regimes. The proposed effects are found to be significant for system parameters of current state-of-the-art photonic-crystal cavities.

DOI: 10.1103/PhysRevB.94.235301

I. INTRODUCTION

Single quantum dots (QDs) in photonic nanostructures have been researched intensely in the last decades as a way to deterministically couple single photons to single emitters for, e.g., quantum-information processing applications [1]. QDs are complex solid-state quantum emitters. They possess internal fine structure in the form of multiple bright and dark exciton states [2], and the lack of parity symmetry even imply that the point dipole approximation becomes invalid in certain nanostructures [3,4]. Furthermore, e.g., photonic crystals (PCs) have highly complex spatial electric field distributions, including a spatially varying polarization. Despite such complexities, it is surprisingly often assumed that a simple two-level description suffices in modeling a QD in a photonic nanostructure, e.g., in the context of cavity quantum electrodynamics (QED) experiments.

We demonstrate that effects of the multilevel structure of QDs may give qualitatively different behavior in PC cavities than is the case for a two-level description. Both the emission dynamics and spectra are significantly modified, which could have direct consequences for a number of previous experimental demonstrations [5–11]. The study adds to the current understanding that the complex near-field polarization effects found in photonic nanostructures lead to new physics, another recent example being that of chiral photon-emitter coupling [12,13]. We emphasize that the discussed effects are likely of relevance also for other types of emitters, e.g., NV centers in diamond or single atoms, where the the complex polarization properties of PC cavities could also lead to effects originating from multiple levels.

We consider the situation of a self-assembled QD positioned in a photonic-crystal cavity, as outlined in Fig. 1. The cavity is assumed to be resonant with the ground-state exciton transition multiplet, which is composed of an electron with a projected angular momentum of $J_z = \pm 1/2$ and a hole with $J_z = \pm 3/2$, resulting in four different exciton states (z is the growth direction of the QD). The states $J_z = \pm 1$ are bright and circularly polarized, while $J_z = \pm 2$ are dark states. However, strain breaks the in-plane symmetry of the exciton wave function, and as a result the bright states mix to form new eigenstates, being positive and negative superpositions of $|\pm 1\rangle$ [2]. The new eigenstates are linearly polarized with a $\pi/2$ phase shift between them, and the degeneracy is lifted with a fine-structure splitting of a few tens of μeV. The two resulting linear dipoles are aligned along the crystalline axes, denoted the x and y axis. The two dark states are a few hundreds of μeV below the bright states [2], and through phonon- and exchange-mediated electron spin-flip processes they each couple to one of the bright states. Due to this spin-flip process the QD decays biexponentially, with the fast (slow) decay rate given by the decay of the bright (dark) exciton states. In the analysis presented here we will neglect the contributions from dark-exciton recombination, which can readily be identified experimentally in a time-resolved experiment [14].

The resulting exciton level scheme is depicted in Fig. 1(a), where the two bright states $|X\rangle_B$ and $|Y\rangle_B$ are linearly polarized transitions oriented along x and y that both can decay to the ground state $|g\rangle$. Each bright exciton state is coupled to the cavity mode with coupling strengths denoted g_x and g_y, respectively, and Δ_x, Δ_y denote the frequency detuning with respect to the cavity. Furthermore, γ is the residual spontaneous-emission rate of the two exciton states for coupling to other modes (assumed to be identical), and κ is the leakage rate of the cavity mode, which is connected to the cavity Q factor by $\kappa = \omega_c/Q$.

In the standard description of QD-cavity QED, the two dipole transitions are assumed to be independent, which holds if the local linear polarization of the cavity field is fully aligned along the axis of one of the dipole orientations. In this case a simple two-level description is sufficient. In the following section we will quantify that this assumption is usually not valid in photonic crystals, because the polarization of the cavity field is strongly dependent on position. More quantitatively, we find that for 44.5% of all positions in the cavity two conditions apply that make the two-level approximation not valid: the cavity field strength is simultaneously large and the primary polarization is off axis, i.e., not along the x or y axes. As a result, both dipoles will generally couple to the same optical mode, and this significantly modifies the spontaneous-emission dynamics, which can be either enhanced or slowed down depending on the exact parameters, which resembles the super- and subradiant behavior found in a multiemitter case.

*lodahl@nbi.ku.dk; www.quantum-photonics.dk

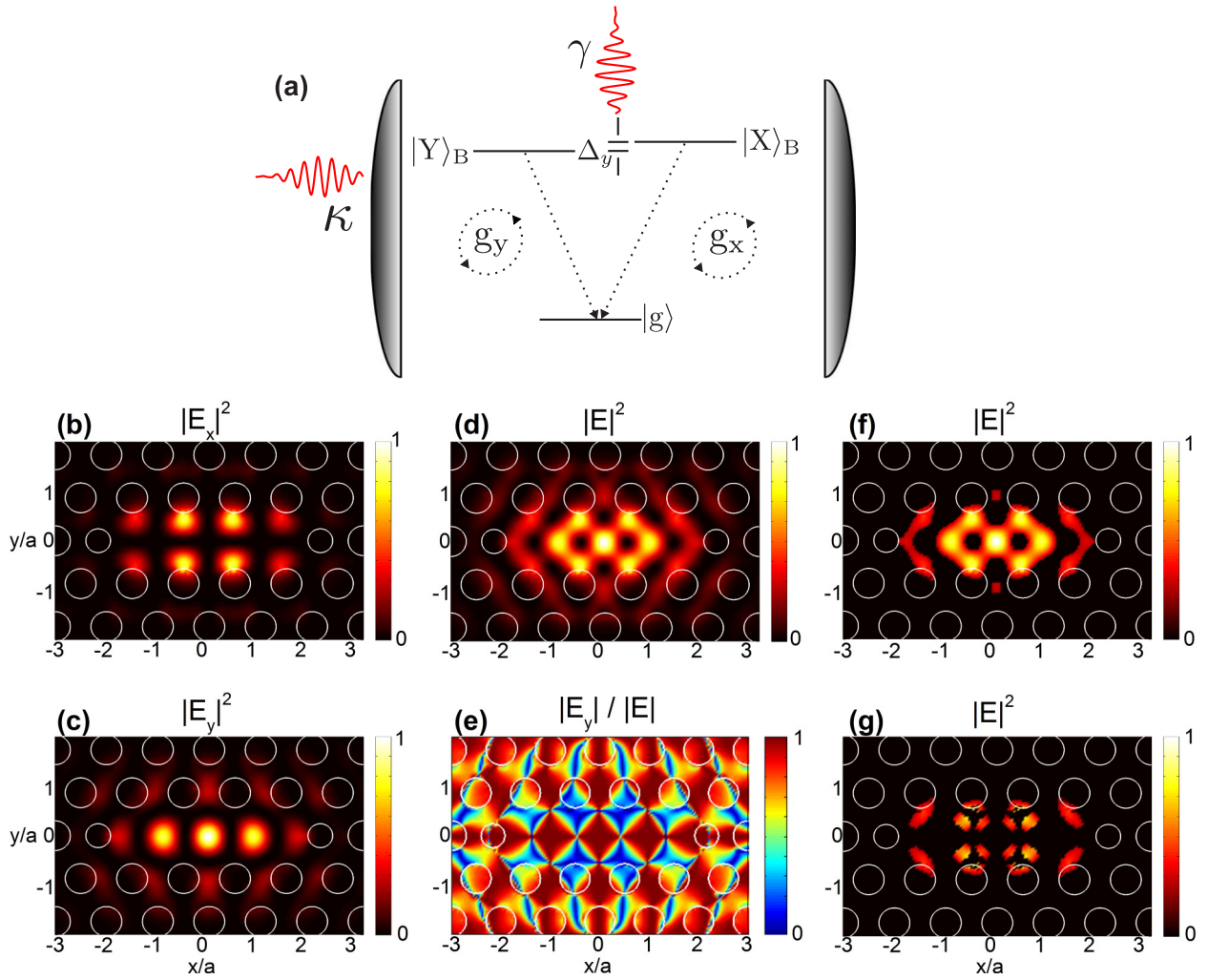

FIG. 1. (a) Energy-level scheme of QD coupled to an optical cavity. The relevant coupling and decay rates are shown. Plots of (b) $|E_x|^2$, (c) $|E_y|^2$, and (d) $|E|^2$ of an empty photonic-crystal cavity with $\lambda_{\text{cav}} = 913$ nm. Clearly, both x and y components of the electric field are present and of comparable strength. (e) Plot of the direction of polarization $|E_y|/|E|$, where 1 (0) corresponds to the total field being $y(x)$ polarized. Many positions inside the cavity are found to exhibit off-axis polarization. (f) Plot of $|E|^2$ where $|E|^2 > 0.25\text{max}(|E|^2)$ is fulfilled. (g) Plot of $|E|^2$ where both $|E|^2 > 0.25\text{max}(|E|^2)$ and $0.2 < |E_y|/|E| < 0.8$ are fulfilled. This plot shows that for many spatial positions the magnitude of the electric field is large (minimum 25% of the maximum value) while the polarization is substantially off-axis (minimum 20%). The white circles indicate the air holes etched in the GaAs membrane. All plots except (e) are normalized to $\text{max}(|E|^2)$.

The discussed phenomena turn out to be remarkably robust to the relevant dephasing processes found in the QD system and are considered to be of high relevance for a number of recent experiments.

II. THE ELECTRIC FIELD OF THE PHOTONIC-CRYSTAL CAVITY

In the present work we consider as a specific example an L3 PC cavity. Importantly, the results are of general relevance, since all field distributions of PC cavities are composed of the same Bloch modes. In Figs. 1(b) and 1(c) we show the magnitude of the two orthogonal polarizations of the electric field on resonance with the highest Q-factor cavity mode. We note that both in-plane components of the electric field, E_x and E_y, are real, and as a consequence the electric field is linearly polarized in the cavity. It is evident that both the magnitude and polarization of the electric field have strong spatial variations. In Fig. 1(d) the magnitude of the total electric field is shown. The polarization of the electric field, i.e., $|E_y|/|E|$, is shown in Fig. 1(e), where a value of 1 (0) denotes polarization along the y (x) axis. Importantly, the off-axis (meaning not aligned to x or y axis) polarization is only of experimental importance if the field strength is also large at these positions. In order to verify that this is indeed the case, we plot $|E|^2$ in Fig. 1(f) at the positions where $|E|^2 > 0.25 \times \text{max}(|E|^2)$ is fulfilled, i.e., where the electric field intensity is more than 25% of the maximum. The corresponding area is found to be $A_1 = 3.057a^2$. Furthermore, Fig. 1(g) is similar to Fig. 1(f) but with the additional requirement that the polarization has to be at least 20% off axis, meaning that $0.2 < |E_y|/|E| < 0.8$. A_2 denotes the area where these two conditions are fulfilled and is found to be $1.360a^2$. In conclusion, this means that for $A_2/A_1 = 44.5\%$ of all the positions, where the cavity field is pronounced, the polarization is also substantially off axis. Thus, off-axis polarization is very abundant in PC cavities.

The immediate consequence is that a QD will generally couple both bright exciton states simultaneously to a cavity mode. We expect this to be relevant for all single QD-cavity QED experiments, irrespective of whether the spatial position of the QD in the cavity is controlled or not. Indeed, in devices containing deterministically positioned QDs, a typical positioning precision of 10% [6] of the lattice constant is achieved, and from Fig. 1(e) it is evident that off-axis coupling and thus multilevel dynamics is likely to play an important role.

III. THE THEORETICAL MODEL

We consider the case of having only a single excitation in the QD-cavity system, which is the relevant setting of many QED experiments. There are four possible states: $|X\rangle_B = |X,0\rangle$, $|Y\rangle_B = |Y,0\rangle$, $|1\rangle = |g,1\rangle$, and $|0\rangle = |g,0\rangle$, where the first (second) position refers to the state of the QD (cavity). The system bears resemblance to the two-emitter model pioneered by [15] where two independent two-level systems are placed within the same cavity [16]. The major difference is that when the QD is in, e.g., the $|X\rangle_b$ state and then the $|Y\rangle_b \rightarrow |1\rangle$ transition is dark, but when $|X\rangle_b$ has decayed into the state $|1\rangle$ then both the $|1\rangle \rightarrow |X\rangle_b$ and $|1\rangle \rightarrow |Y\rangle_b$ transitions are active. This can be thought of as a time-dependent coupling strength and is not present in the two-emitter case.

Having made the dipole and rotating-wave approximation, the Hamiltonian in the rotating frame can be written

$$\hat{H} = \hbar\Delta_x\hat{\rho}_{xx} + \hbar\Delta_y\hat{\rho}_{yy} + \hbar(g_x\hat{\rho}_{x1} + g_x^*\hat{\rho}_{1x}) + \hbar(g_y\hat{\rho}_{y1} + g_y^*\hat{\rho}_{1y}), \quad (1)$$

where the operators are defined as $\hat{\rho}_{ij} = |i\rangle\langle j|$. In order to include dissipation we write the master equation for the density matrix operator as [17]

$$\dot{\hat{\rho}} = -i\hbar^{-1}[\hat{H},\hat{\rho}] + \hat{L}(\kappa,\hat{\rho}_{01}) + \hat{L}(\gamma,\hat{\rho}_{0x}) + \hat{L}(\gamma,\hat{\rho}_{0y}) + \hat{L}(2\gamma_{\rm dp},\hat{\rho}_{00}+\hat{\rho}_{11}), \quad (2)$$

where $\hat{L}$ denotes a Lindblad operator defined as $\hat{L}(\Gamma,\hat{R}) = \Gamma(\hat{R}\hat{\rho}\hat{R}^\dagger - \frac{1}{2}\hat{R}^\dagger\hat{R}\hat{\rho} - \frac{1}{2}\hat{\rho}\hat{R}^\dagger\hat{R})$. The first three Lindblad terms give the decay of the cavity due to the finite Q factor, the decay of the x dipole, and of the y dipole out of the cavity, respectively. The fourth Lindblad term models pure dephasing caused by the solid-state environment. Based on experimental work [18], we include a pure dephasing rate that dephases the two bright states with respect to the ground state but keeps the mutual coherence between the states. We consider the experimentally relevant situation of nonresonant excitation and limit to a single excitation in the system and therefore assume that the initial populations of the x and y states are the same, i.e., $\rho_{\rm x}(0) = \rho_{\rm y}(0) = 1/2$, where $\rho_{\rm x}$ and $\rho_{\rm y}$ denote the populations of the x- and y-polarized dipoles. The QD is thus prepared in a mixed state. For all the following results we use the realistic parameters [19] $\kappa = 198/\hbar\ \mu$eV $= 47.9$ GHz, $\gamma = 0.2/\hbar\ \mu$eV $= 48.4$ MHz, $\gamma_{\rm dp} = 0.1/\hbar\ \mu$eV $= 24.2$ MHz, and a fine-structure splitting of $10/\hbar\ \mu$eV $= 2.4$ GHz, i.e., $\hbar\Delta_y = \hbar\Delta_x + 10/\hbar\ \mu$eV. The two linear dipole transitions are formed as superpositions of two circular dipoles, and as a result there is a $\pi/2$ phase difference between the two linear dipoles.

IV. WEAK-COUPLING REGIME

Although the influence of the two bright states is intuitively clear in the weak-coupling regime, we still briefly discuss this regime due to the relevance to experiments. When performing experiments, the measured observable is the population of the QD. The coherent state of the QD can be written as $|\Psi_{\rm coh}\rangle = |X\rangle_B + |Y\rangle_B$. We construct the operator according to the coherent sum $\hat{\rho}_{\rm coh} = |\Psi_{\rm coh}\rangle\langle\Psi_{\rm coh}| = \hat{\rho}_{xx} + \hat{\rho}_{yy} + \hat{\rho}_{xy} + \hat{\rho}_{yx}$.

The weak-coupling regime is well known from the standard theory of cavity QED, where a single dipole within a cavity is considered. In that case the cavity enhances the decay rate of the dipole, but the decay remains irreversible. In the present case of two dipole transitions coupled to the same cavity mode a similar result is obtained. The only significant difference is that two-dipole interference can occur. Due to the nonresonant excitation considered here, the initial state of the QD is in a mixed state. Therefore, there is no coherence between the two dipoles initially, and since the decay is irreversible, no coherence is built over time. The recombination of the bright exciton therefore gives rise to a biexponential decay with the two decay rates being proportional to g_x and g_y, respectively. In the weak-coupling regime, the V-level system can thus be considered two separate two-level systems. In a comparison with experiments one must also account for dark exciton states. As a result, the experimentally predicted decay curve would be a triple exponential, where two of the decay rates depend on the local density of optical states (LDOS), while the latter depends on the (nonradiative) recombination of dark excitons [14].

V. STRONG-COUPLING REGIME

The strong-coupling regime is characterized by a reversible decay, which in contrast to the weak-coupling regime allows the mutual coherence between the two dipole transitions to build up over time. This gives rise to new mixed eigenstates, i.e., the two transitions cannot be treated independently. In Fig. 2(a) the population of the x dipole (ρ_x), y dipole (ρ_y), and the coherent sum ($\rho_{\rm coh}$) is plotted as a function of time with the parameters $\hbar g_x = 100\ \mu eV$ and $g_y = i0.1g_x$. This corresponds to the x transition being strongly coupled, while the y transition is weakly coupled. The populations ρ_x and ρ_y start at $1/2$ due to the initial conditions, and as expected the decay of ρ_x shows Rabi oscillations while ρ_y approximately decays with the background decay rate γ. The Rabi oscillation of ρ_x agrees well with that expected for a two-level model of the x transition, cf. curve labeled $\rho_x^{2-\rm level}$. However, a single two-level system with the same coupling strength gives a significantly faster decay rate than the full model. In an experiment neither ρ_x nor ρ_y is recorded but rather the coherent sum $\rho_{\rm coh}$. It is seen to decay from unity to $1/2$, where it exhibits a small oscillation before decaying from $1/2$ to 0 with approximately the background decay rate γ. This behavior is qualitatively different from the case of independent two-level systems.

In Figs. 2(b) and 2(c) the coupling strength is increased to $g_y = ig_x/2$ and $g_y = i \times g_x$. While the populations ρ_x

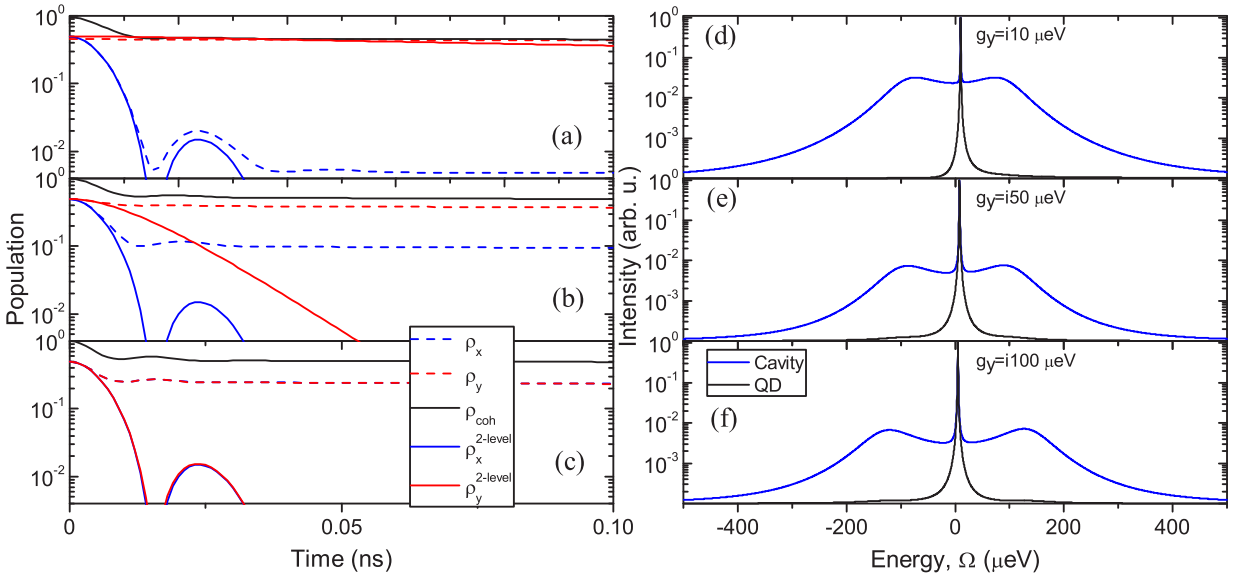

FIG. 2. (a–c) The population decay of the x dipole (ρ_x), y dipole (ρ_y), and the coherent sum (ρ_{coh}) for $g_x = 100/\hbar\ \mu\text{eV} = 24.2$ GHz and increasing $g_y/g_x = \{i/10\ ,i/2\ ,1i\}$. ρ_{coh} is an experimentally observable quantity, and its slow decay even for $g_y = g_x$ is a testimony of quantum-interference effects. $\rho_x^{2-\text{level}}$ ($\rho_y^{2-\text{level}}$) denotes the population of a corresponding two-level emitter with the same coupling parameters as above. (d–f) Cavity and QD spectra. For a small value of g_y/g_x the cavity spectrum displays a Rabi splitting due to the Rabi oscillations between the x dipole and the cavity. The QD spectrum consists of a narrow single peak due to the slow decay of the y dipole with no sign of Rabi splitting.

and ρ_y exhibit small oscillations before decaying slowly, the experimentally observable coherent sum ρ_{coh} displays a subradiant type of behavior, where it decays from 1 to 1/2 with a single small oscillation before decaying from 1/2 to 0 with a rate γ_{coh}, which approximately takes on the value of the background decay rate γ.

Figures 2(d)–2(f) show the emission spectra consisting of the emission leaking out from the QD (hereby named the QD spectrum) and the emission leaking out of the cavity (named the cavity spectrum). The cavity (QD) spectrum is calculated as the Fourier transform of the two-time correlation function $\langle\hat{\rho_{10}}(t'+\tau)\hat{\rho_{01}}(t')\rangle$ $[\langle[\hat{\rho}_{\text{x0}}(t'+\tau)+\hat{\rho}_{\text{y0}}(t'+\tau)][\hat{\rho}_{\text{0x}}(t')+\hat{\rho}_{\text{0y}}(t')]\rangle]$. The cavity spectrum depends on only the fraction of light that couples to the cavity. For that reason it exhibits a Rabi splitting of $\Omega_R = \sqrt{4(|g_x|^2+|g_y|^2)-(\kappa-\gamma)^2/4}$, i.e., similar to the case of two independent emitters. For the QD spectrum, however, the contrary is the case. The QD spectrum describes the emission that leaks out from the QD without first being emitted into the cavity mode. When $|g_y|$ is large, the slowly decaying state is formed, which does not interact with the cavity. Consequently, all of the emission from this state therefore is in the QD spectrum. The subradiant part decays slowly with the rate γ_{coh}, and as a direct consequence the spectrum is a Lorentzian. These departures from the two-level emitter behavior should be a signature that could be resolved experimentally. However, to our knowledge no experiments to date have resolved the vacuum Rabi splitting for a PC cavity fed by only a single QD to such a precision that the predicted effects have been observed.

In Figs. 3(a) and 3(b) we investigate how the rate γ_{coh} depends on the fine-structure splitting Δ_{y} and on the dephasing rate γ_{dp}, respectively. For small values of the detuning, γ_{coh} increases quadratically and changes to a linear dependence for larger detunings. A slow γ_{coh} is a result of destructive interference, which becomes less and less pronounced with increasing detuning. Figure 3(b) shows that γ_{coh} is independent of the dephasing rate γ_{dp}. This noticeable feature occurs because both bright states are subject to the same dephasing rate, and they thus remain mutually coherent. Dephasing robust long-lived states thus appear naturally in this system. It should be mentioned that slow spectral diffusion processes are often found when applying nonresonant excitation of QDs, which is

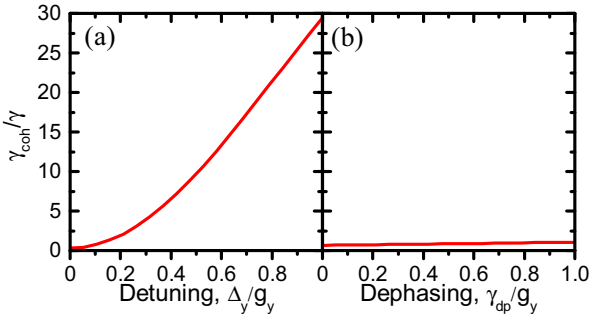

FIG. 3. The decay rate of coherent sum of the population (γ_{coh}) as a function of (a) the detuning, Δ_{y}, between the two bright states in units of the coupling strength g_y and (b) the dephasing rate γ_{dp}. When Δ_{y} increases, the destructive interference responsible for the slow decay disappears and γ_{coh} increases, while it is independent of the dephasing rate γ_{dp}. The following parameters have been used: $g_x = g_y = 100/\hbar\ \mu\text{eV} = 24.2$ GHz, $\Gamma = 0.2/\hbar\ \mu\text{eV} = 48.4$ MHz, $\gamma_{\text{dp}} = 0.2/\hbar\ \mu\text{eV} = 48.4$ MHz for (a) and $g_x = g_y = 100/\hbar\ \mu\text{eV} = 24.2$ GHz, $\Gamma = 0.2/\hbar\ \mu\text{eV} = 48.4$ MHz, $\Delta_{\text{y}} = 10/\hbar\ \mu\text{eV} = 2.4$ GHz, for (b) at $\lambda_{\text{cav}} = 913$ nm.

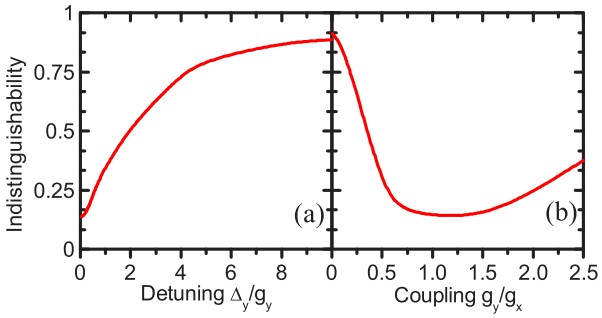

FIG. 4. The indistinguishability as a function of (a) the detuning, Δ_y, between the two bright states in units of the coupling strength g_y and (b) the coupling strength g_y. At small Δ_y the slowly decaying state causes a prolonged lifetime, which reduces the degree of indistinguishability. The values of the additional parameters are identical to the case of Fig. 3.

not accounted for in the analysis. However, spectral diffusion occurs on a time scale much longer than the exciton coherence dynamics [20] and therefore leads only to a spectral broadening of the emission spectra and does not influence the dynamics. Furthermore, we consider here the case of symmetric coupling ($g_x = g_y$), while any asymmetry will lead to a faster γ_{coh}.

A QD embedded in PC structures is a potential source of photonic qubits to be utilized in quantum-information processing. An important benchmark of a photon source is the coherence of the emitted photons. This is characterized by the degree of interference of two photons, called the indistinguishability [21]. The indistinguishability of a single two-level system in the weak-coupling regime is determined by the radiative decay rate Γ and the dephasing rate γ_{dp} through $V = \frac{\Gamma}{\Gamma+2\gamma_{\mathrm{dp}}}$ [22]. If the emitter is interacting with a cavity mode, the indistinguishability can be improved through the Purcell effect, since the radiative rate is enhanced by the cavity. In the weak-coupling regime the addition of a second transition will cause a reduction of the indistinguishability, since quantum interference is reduced due to the two different transitions. In the following we will focus on the strong-coupling regime, where the above simple expression for the indistinguishability is not valid and the general theory of Ref. [21] needs to be applied. In Fig. 4(a) we show the indistinguishability as a function of the fine-structure splitting, where $|g_y| = |g_x|$. Surprisingly the indistinguishability is low for zero detuning, even though the fine-structure splitting does not reduce it. The explanation for this can be found in Fig. 3(a). At zero detuning the system is in a slowly decaying state and is therefore susceptible to dephasing. As the fine-structure splitting increases the indistinguishability increases as a consequence of the break up of the slowly decaying state. In Fig. 4(b) we show the indistinguishability as a function of the coupling strength of the y-dipole g_y, where the detuning is $\Delta_y = 10\ \mu eV$. When the y-dipole is uncoupled, $g_y = 0$ the indistinguishability is close to unity, since the x dipole is strongly coupled to the cavity. As the coupling strength of the y dipole increases, the slowly decaying state forms and the indistinguishability is reduced until the two coupling strengths are equal. As g_y exceeds g_x the slowly decaying state deteriorates, causing the indistinguishability to increase.

VI. CONCLUSION

In conclusion, we have shown that the fine structure of QDs may play a significant role for cavity QED experiments in photonic crystals. Quantitative simulations show that the electric field of the cavity couples substantially to both dipole transitions in more than 40% of all the possible QD positions. In the weak-coupling regime, the coupling to both dipoles gives rise to two detuning-dependent decay rates. In the strong-coupling regime, a long-lived hybridized state is formed, which quantitatively modifies the emission dynamics and spectrum. The slowly decaying state is predicted to be insensitive to decoherence of the QD level scheme. We believe that the predicted behavior is readily observable in a quantitative cavity QED experiment with QDs in photonic crystals and may already play a role in existing experiments reported in the literature.

ACKNOWLEDGMENTS

We thank S. Mahmoodian, I. Söllner, and A. Sørensen for fruitful discussion. We gratefully acknowledge financial support from the the Danish Council for Independent Research (Natural Sciences and Technology and Production Sciences) and the European Research Council (ERC Consolidator Grant–ALLQUANTUM).

[1] P. Lodahl, S. Mahmoodian, and S. Stobbe, Rev. Mod. Phys. **87**, 347 (2015).
[2] M. Bayer, G. Ortner, O. Stern, A. Kuther, A. A. Gorbunov, A. Forchel, P. Hawrylak, S. Fafard, K. Hinzer, T. L. Reinecke, S. N. Walck, J. P. Reithmaier, F. Klopf, and F. Schäfer, Phys. Rev. B **65**, 195315 (2002).
[3] M. L. Andersen, S. Stobbe, A. S. Sørensen, and P. Lodahl, Nat. Phys. **7**, 215 (2011).
[4] P. Tighineanu, A. S. Sørensen, S. Stobbe, and P. Lodahl, Phys. Rev. Lett. **114**, 247401 (2015).
[5] T. Yoshie, A. Scherer, J. Hendrickson, G. Khitrova, H. M. Gibbs, G. Rupper, C. Ell, O. B. Shchekin, and D. G. Deppe, Nature (London) **432**, 200 (2004).
[6] K. Hennessy, A. Badolato, M. Winger, D. Gerace, M. Atatüre, S. Gulde, S. Fält, E. L. Hu, and A. Imamoğlu, Nature (London) **445**, 896 (2007).
[7] A. Laucht, N. Hauke, J. M. Villas-Bôas, F. Hofbauer, G. Böhm, M. Kaniber, and J. J. Finley, Phys. Rev. Lett. **103**, 087405 (2009).
[8] Y. Ota, M. Shirane, M. Nomura, N. Kumagai, S. Ishida, S. Iwamoto, S. Yorozu, and Y. Arakawa, Appl. Phys. Lett. **94**, 033102 (2009).
[9] D. Englund, A. Majumdar, A. Faraon, M. Toishi, N. Stoltz, P. Petroff, and J. Vučković, Phys. Rev. Lett. **104**, 073904 (2010).
[10] A. Faraon, I. Fushman, D. Englund, N. Stoltz, P. Petroff, and J. Vučković, Nat. Phys. **4**, 859 (2008).

[11] A. Reinhard, T. Volz, M. Winger, A. Badolato, K. J. Hennessy, E. L. Hu, and A. Imamoğlu, Nat. Photonics. **6**, 93 (2012).
[12] C. Junge, D. O'Shea, J. Volz, and A. Rauschenbeutel, Phys. Rev. Lett. **110**, 213604 (2013).
[13] I. Söllner, S. Mahmoodian, S. L. Hansen, L. Midolo, A. Javadi, G. Kiršanskė, T. Pregnolato, H. El-Ella, E. H. Lee, J. D. Song, S. Stobbe, and P. Lodahl, Nat. Nanotechnol. **10**, 775 (2015).
[14] J. Johansen, B. Julsgaard, S. Stobbe, J. M. Hvam, and P. Lodahl, Phys. Rev. B **81**, 081304 (2010).
[15] R. H. Dicke, Phys. Rev. **93**, 99 (1954).
[16] M. Tavis and F. W. Cummings, Phys. Rev. **170**, 379 (1968).
[17] H. J. Carmichael, R. J. Brecha, M. G. Raizen, H. J. Kimble, and P. R. Rice, Phys. Rev. A **40**, 5516 (1989).
[18] A. J. Hudson, R. M. Stevenson, A. J. Bennett, R. J. Young, C. A. Nicoll, P. Atkinson, K. Cooper, D. A. Ritchie, and A. J. Shields, Phys. Rev. Lett. **99**, 266802 (2007).
[19] K. H. Madsen and P. Lodahl, New J. Phys. **15**, 025013 (2013).
[20] A. V. Kuhlmann, J. Houel, A. Ludwig, L. Greuter, D. Reuter, A. D. Wieck, M. Poggio, and R. J. Warburton, Nat. Phys. **9**, 570 (2013).
[21] A. Kiraz, M. Atatüre, and A. Imamoğlu, Phys. Rev. A **69**, 032305 (2004).
[22] J. Bylander, I. Robert-Philip, and I. Abram, Eur. Phys. J. D **22**, 295 (2003).